

# THE COMPOSITION OF COSMIC RAYS AT THE KNEE <sup>1</sup>

JÖRG R. HÖRANDEL

University of Karlsruhe, Institut für Experimentelle Kernphysik,  
PO Box 3640, 76021 Karlsruhe, Germany — [www-ik.fzk.de/~joerg](http://www-ik.fzk.de/~joerg)

## Abstract

The present experimental status concerning the composition of cosmic rays in the PeV region is reviewed. The results are compared to predictions of contemporary models for the acceleration and propagation of galactic cosmic rays.

## 1 Introduction

The solar system is permanently exposed to a vast flux of highly energetic and fully ionized atomic nuclei, the cosmic rays. Their energies extend from the GeV range to at least  $10^{20}$  eV. Over a wide range the energy spectrum follows a power law  $dN/dE \propto E^\gamma$ . The spectral index changes around 4 PeV from  $\gamma \approx -2.7$  to  $\gamma \approx -3.1$ . This transition phenomenon has been reported for the first time in 1958 [1] and is commonly referred to as *the knee*. A cutout of the energy spectrum in the knee region is depicted in Fig. 1. Shown is the all-particle energy spectrum, which exhibits the knee, as well as results from direct measurements above the atmosphere for primary protons and iron nuclei.

The origin of the knee is one of the central questions of high-energy astroparticle physics, closely related to the mechanisms of acceleration and propagation of high-energy cosmic rays. Answers are expected from the

---

<sup>1</sup>Invited talk, presented at the Workshop on Frontier Objects in Astrophysics and Particle Physics, Vulcano, May 24<sup>th</sup> - 29<sup>th</sup>, 2004.

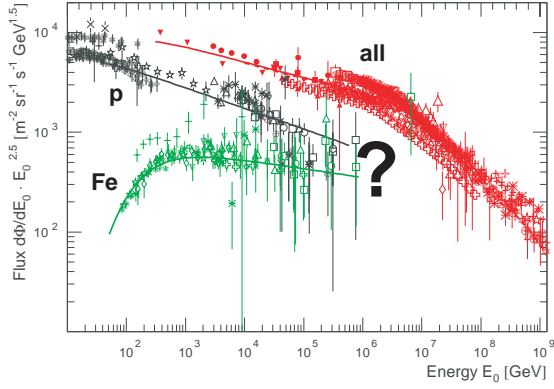


Figure 1: Energy spectrum of cosmic rays for all particles (dark grey), protons (black), and iron nuclei (light grey), for references see [2].

measurements of the energy spectra for individual elements (or at least elemental groups) above 1 PeV. Since this is an extreme experimental challenge, one often measures the average atomic mass instead.

In this article, the present experimental status is reviewed and the results are set in context to predictions of contemporary models for the acceleration and propagation of cosmic rays.

Ideally, one would like to continue the energy spectra for individual elements above several  $10^{14}$  eV with direct measurements above the atmosphere. At present, several groups measure in this region, applying different experimental techniques, e.g. a calorimeter (ATIC [3]) or a transition radiation detector (TRACER [4]). The TRACER experiment, investigating nuclei from oxygen to iron, had a 14 day flight from Mc Murdo, Antarctica in December 2003. Recent accelerator tests have shown that transition radiation detectors can be utilized to measure energy spectra of cosmic rays in a space borne experiment up to energies of about 1 PeV/n [5].

Presently, at energies above 1 PeV one relies on indirect measurements. In these experiments the secondary products, generated by interactions of cosmic-ray particles with nuclei in the atmosphere are investigated. Two basic approaches can be distinguished: Measuring the debris of the particle cascade at ground level by registering electrons, muons, or hadrons. Or measuring the longitudinal shower development in the atmosphere by exploration of the Čerenkov or Fluorescence light generated predominantly by the shower electrons. An astrophysical interpretation of air shower data requires detailed knowledge of the interaction processes in the atmosphere. One of the tasks of air shower experiments is to improve the understanding of high-energy interactions above the energies covered by todays accelerator experiments and beyond their kinematical bound, see e.g. [6].

## 2 Origin of the knee

The bulk of cosmic rays is assumed to be accelerated in shock fronts of supernova remnants (SNRs). This goes back to an idea of Baade and Zwicky, who have estimated the total power required to generate the observed flux of cosmic rays [7]. It can be shown, that about 3 supernovae per galaxy and century are sufficient to release enough kinetic energy in order to deliver the required power. A mechanism to accelerate particles by moving magnetic clouds has been introduced by Fermi [8]. The present understanding of acceleration in strong shock fronts has been initiated by Blanford and Ostriker [9] which could demonstrate that at strong shocks particles are accelerated efficiently. The finite lifetime of a shock front ( $\sim 10^5$  a) limits the maximum energy attainable to  $E_{max} \sim Z \cdot (0.1 - 5)$  PeV for particles with charge  $Z$ . Various versions of this scenario have been discussed, see e.g. [10, 11, 12, 13, 14]. In the literature also other possibilities, like the acceleration of particles in  $\gamma$ -ray bursts are discussed [15, 16].

After acceleration, the particles propagate in a diffusive process for about  $20 \cdot 10^6$  a through the Galaxy, being deflected many times by the randomly oriented galactic magnetic fields ( $B \sim 3 \mu\text{G}$ ). The propagation is accompanied by leakage of particles out of the Galaxy. With increasing energy it is more and more difficult to magnetically bind the nuclei to the Galaxy. The pathlength of traversed material decreases as  $\Lambda \propto E^\delta$ , with  $\delta \approx -0.6$ . Many approaches have been undertaken to describe the propagation process, see [17, 18, 19, 20, 21]. During the propagation phase, reacceleration of particles has been suggested at shock fronts originating from the galactic wind [22].

Both, the acceleration and the propagation/leakage processes are expected to yield cut-offs for the fluxes of nuclei at energies proportional to their nuclear charge  $E_k \propto Z$ .

As further possible causes for the knee, interactions of cosmic-ray nuclei with background photons or neutrinos in the Galaxy [23, 24, 25] or new types of interactions in the atmosphere [26] have been discussed. For a more comprehensive review of models the reader is referred to [27].

Electromagnetic emission of SNR has been detected in a wide energy range from radio wave lengths to the x-ray regime. The observations can be interpreted as synchrotron emission from electrons, which are accelerated in these regions [29]. Recently, the HEGRA experiments has detected an excess of high-energy  $\gamma$ -rays from the supernova remnant Cas A, see Fig. 2. This is interpreted as evidence for hadron acceleration in the SNR. The hadrons interact with protons of the interstellar medium, producing  $\pi^0$ s, which decay into high-energy photons, supposedly detected by the HEGRA

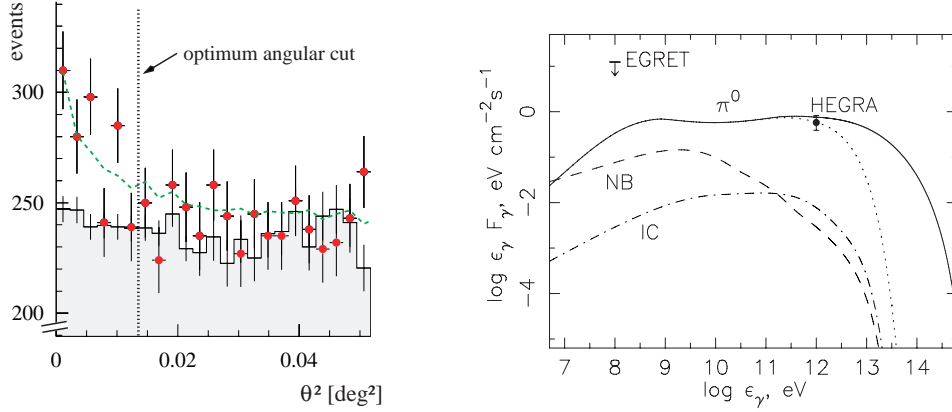


Figure 2: Left: The dots indicate the measured  $\gamma$ -ray signal as function of angular distance to Cassiopeia A as measured by the HEGRA experiment. The shaded area is a background estimate [28]. Right: Integral  $\gamma$ -ray fluxes due to inverse Compton scattering, non-thermal bremsstrahlung and  $\pi^0$ -decay according to the model by Berezhko et al. compared with measurements of the HEGRA and EGRET experiments [29]. The dotted line is obtained for an assumed cut-off at 4 TeV.

experiment [29]. The flux is compatible with a model of electron and hadron acceleration in shock fronts, see Fig. 2.

Recently, an excess of charged particles from the direction of a SNR (Monogem ring,  $d \approx 300$  pc) has been reported [30]. However, such a signal could not be confirmed by the KASCADE experiment [31]. The latter has performed a detailed search for point sources, covering the whole visible sky at energies  $E_0 > 0.3$  PeV. Special attention has been given to the region of the galactic plane, as well as to the vicinity of known SNRs and TeV- $\gamma$ -ray sources. No significant excess could be found. The gyromagnetic radius<sup>2</sup> of particles with an energy around 1 PeV in the galactic magnetic field is in the order of 1 pc. Hence, it is not expected to find any point sources at these energies.

To characterize the large scale anisotropy of cosmic rays, the Rayleigh amplitude

$$A = \sqrt{\left( \frac{2}{n} \sum_{i=1}^n \sin \alpha_i \right)^2 + \left( \frac{2}{n} \sum_{i=1}^n \cos \alpha_i \right)^2}$$

for  $n$  events which are detected at a right ascension angle  $\alpha_i$  is introduced. A compilation of measured amplitudes as function of energy is given in Fig. 3 [32]. An increase of  $A$  as function of energy can be recognized. This trend

<sup>2</sup> $r_G = p/(ZeB)$  for a particle with momentum  $p$  and charge  $Ze$  in a magnetic field  $B$ .

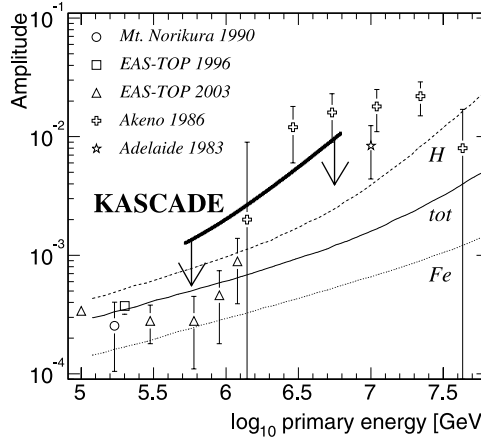


Figure 3: Rayleigh amplitudes as function of energy for various experiments, for references see [32]. Additionally, model predictions for a diffusion model are shown. The lines indicate the expected anisotropy for primary protons (H) and iron nuclei (Fe) as well as for all particles (tot) [33].

is compatible with expectations taking into account diffusive propagation of cosmic rays in the Galaxy [33], as indicated by the lines.

### 3 Energy spectrum of cosmic rays

The all-particle energy spectrum has been derived by many experiments as shown in Fig. 4. In this representation the flux of the air shower experiments has been normalized to the extrapolated flux of direct measurements at 1 PeV by introducing a slight adjustment ( $\pm 10\%$ ) of the energy scales of the individual experiments [2]. It is quite interesting to realize that the absolute energy calibration of these various experiments, using different observation techniques and models to describe the shower development in the atmosphere agree within  $\pm 10\%$ . The normalized all-particle flux changes smoothly without any prominent structures. The solid and dotted lines in-

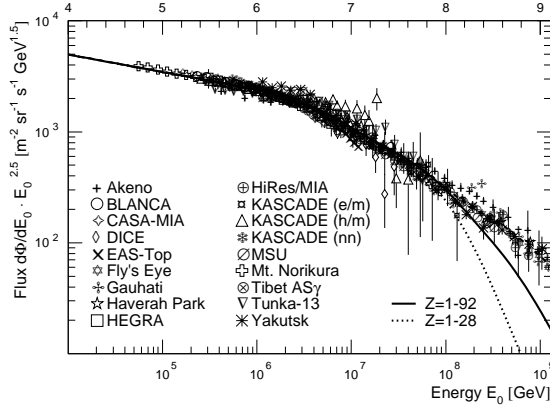


Figure 4: Normalized all-particle energy spectra for individual experiments, for details and references see [2].

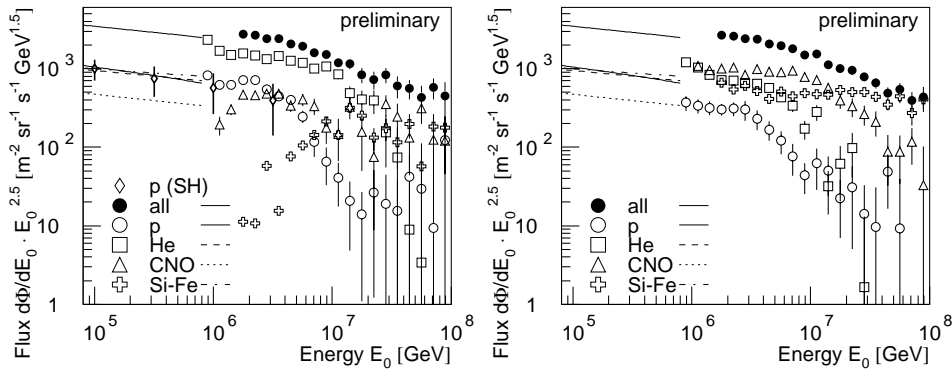


Figure 5: Results from the KASCADE experiment: Energy spectra for groups of elements derived from the data using CORSIKA with the hadronic interaction models QGSJET (left) and SIBYLL (right) [34]. In addition, the proton spectrum as derived from the measurements of single hadrons is shown [35]. The lines indicate extrapolations of direct measurements [2].

dicate the total sum of galactic cosmic rays according to a parameterization of data [2].

The KASCADE group performed systematic studies to evaluate the influence of different hadronic interaction models used in the simulations to interpret the data on the resulting spectra for elemental groups [34]. Two sets of spectra, derived from the observation of the electromagnetic and muonic air shower components, applying the Gold algorithm and using CORSIKA [37] with the hadronic interaction models QGSJET and SIBYLL are compiled in Figure 5.

As can be seen in the figure, the flux for elemental groups depends on the model used. The KASCADE group emphasizes that at present, there are systematic differences between measured and simulated observables, which result in the ambiguities of the spectra for elemental groups. These conclusions apply in a similar way also to other experiments. A correct deconvolution of energy spectra for elemental groups requires a precise knowledge of the hadronic interactions in the atmosphere. The interaction models presently used do not describe the measurements with a sufficiently high precision required for this task.

The figure also shows the spectrum of primary protons, which has been derived from the flux of unaccompanied hadrons [35]. The spectrum is compatible with the proton flux as obtained from the unfolding procedure when using the QGSJET model. For comparison, also the results of direct measurements at lower energies at the top of the atmosphere [2] are presented in the figure.

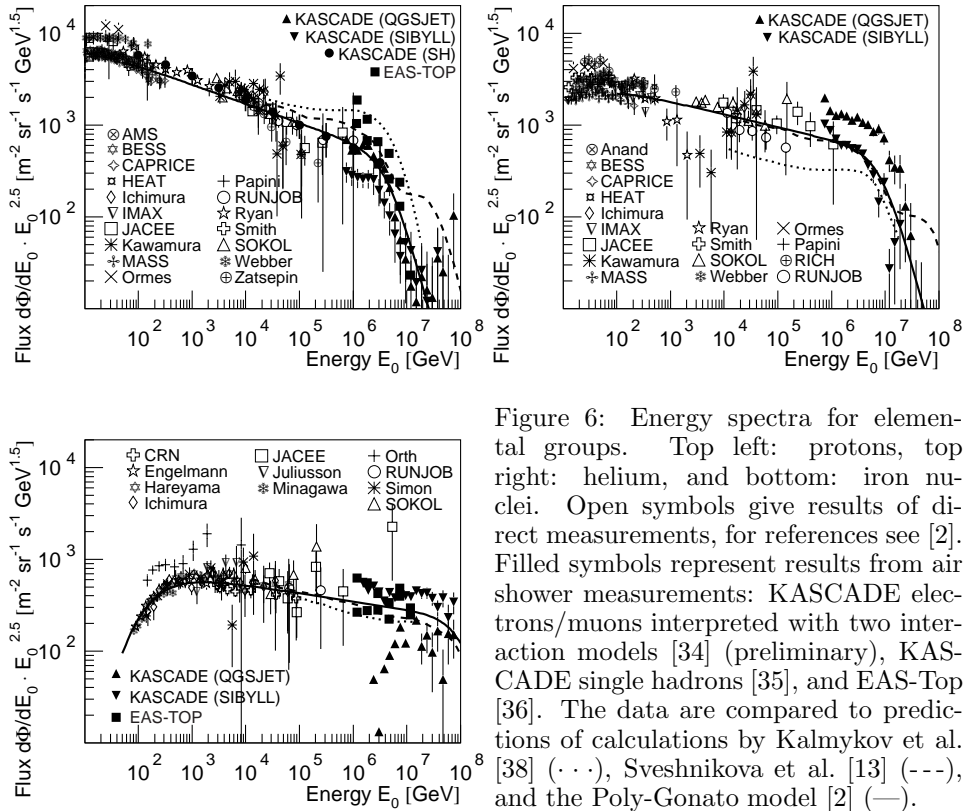


Figure 6: Energy spectra for elemental groups. Top left: protons, top right: helium, and bottom: iron nuclei. Open symbols give results of direct measurements, for references see [2]. Filled symbols represent results from air shower measurements: KASCADE electrons/muons interpreted with two interaction models [34] (preliminary), KASCADE single hadrons [35], and EAS-Top [36]. The data are compared to predictions of calculations by Kalmykov et al. [38] (···), Sveshnikova et al. [13] (---), and the Poly-Gonato model [2] (—).

In order to give an impression of the present status, the energy spectra for three elemental groups (protons, helium, and iron nuclei) are compiled in Fig. 6 over a wide energy range. Shown are results from direct measurements above the atmosphere as well as the KASCADE results described above. The EAS-TOP experiment published two sets of spectra with different assumptions about the contribution of protons and helium nuclei, for details see [36]. The resulting fluxes are indicated by two squares per primary energy. To guide the eye, the solid lines indicate power law spectra with a cut-off at  $Z \cdot 4.5$  PeV. For the iron spectrum at low energies the influence of modulation due to the magnetic fields of the heliosphere can be recognized.

The dashed lines represent calculations of energy spectra for nuclei accelerated in supernova remnants by Sveshnikova et al. [13]. It is assumed that the particles are accelerated in a variety of supernovae populations, each having an individual maximum energy to be attained during acceleration, which results in the bumpy structure of the obtained spectra. The dotted

lines reflect calculations of the diffusive propagation of particles through the Galaxy by Kalmykov et al. [38]. The leakage of particles yields a rigidity dependent cut-off. Comparison with the data may suggest a *qualitative* understanding of the energy spectra. However, for a precise *quantitative* understanding, detailed investigations of the systematic errors of the measurements are necessary and the description of the interaction processes in the atmosphere needs to be improved.

## 4 Mass composition of cosmic rays

The position of the maximum of an electromagnetic or nuclear cascade in matter depends on the incident particles energy as  $X_{max} \propto \ln E_n$ , where  $E_n$  is the energy per nucleon  $E_n = E_0/A$ . Hence,  $X_{max}$  depends on  $\ln A$ . Also, many other observables in air showers like the number of electrons, muons, or hadrons observed at ground level depend roughly on  $\ln A$ . To characterize the cosmic-ray mass composition one uses commonly the mean logarithmic mass  $\langle \ln A \rangle$ , defined as  $\langle \ln A \rangle = \sum r_i \ln A_i$ , where  $r_i$  is the relative fraction of nuclei with atomic mass number  $A_i$ .

The mean logarithmic mass from experiments measuring electrons, muons, and hadrons at ground level using mostly CORSIKA/QGSJET to interpret the data are compiled in Fig. 7c. One recognizes an increase of  $\langle \ln A \rangle$  as function of energy, the line indicates an increase as expected for a rigidity dependent cut-off for individual elements [2].

A second group of experiments measures the average depth of the shower maximum  $X_{max}$  in the atmosphere by registering Čerenkov photons or fluorescence light. Interpreting this data with CORSIKA/QGSJET 01 leads to the results shown in Fig. 7a. An increase of  $\langle \ln A \rangle$  as described before is not obtained.

The description of hadronic interactions within the models is based on accelerator measurements. However, extrapolating the experimental uncertainties to higher energies may cause significant differences in the interpretation of air shower data. For example, the cross sections for proton - anti proton collisions at the Tevatron ( $\sqrt{s} = 1.8$  TeV) exhibit an error of about 10%. To investigate the influence of such uncertainties on the development of air showers, in the model QGSJET 01 the cross section for  $p\bar{p}$  collisions has been reduced to the lower error boundary of the Tevatron data. This results in a deeper penetration of showers into the atmosphere. Accordingly,  $\langle \ln A \rangle$  derived with such an interaction model, using the same experimental  $X_{max}$ -values as before, yields larger values at high energies, as shown

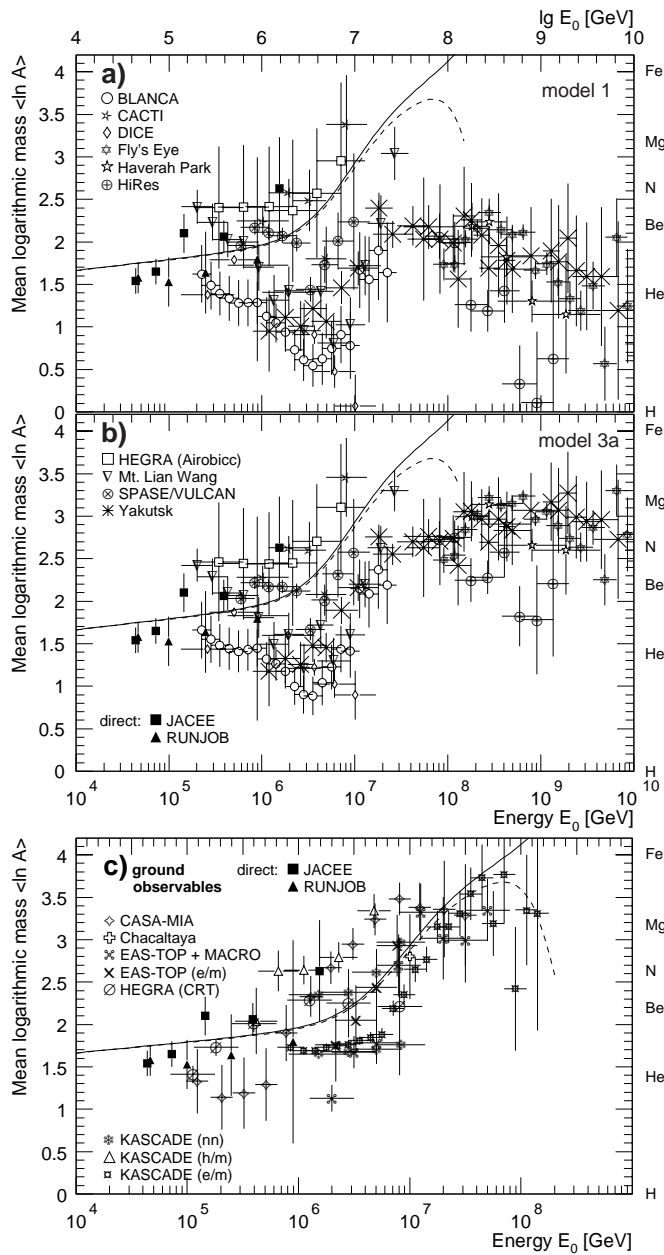


Figure 7: Mean logarithmic mass as function of energy as obtained by various experiments. Top:  $\langle \ln A \rangle$  derived from observations of the average depth of the shower maximum  $X_{\max}$  interpreted with CORSIKA/QGSJET01 (a) and with a modified version (b) [39]. Bottom: Experiments measuring electrons, muons, and hadrons at ground level. For details and references see [2, 39].

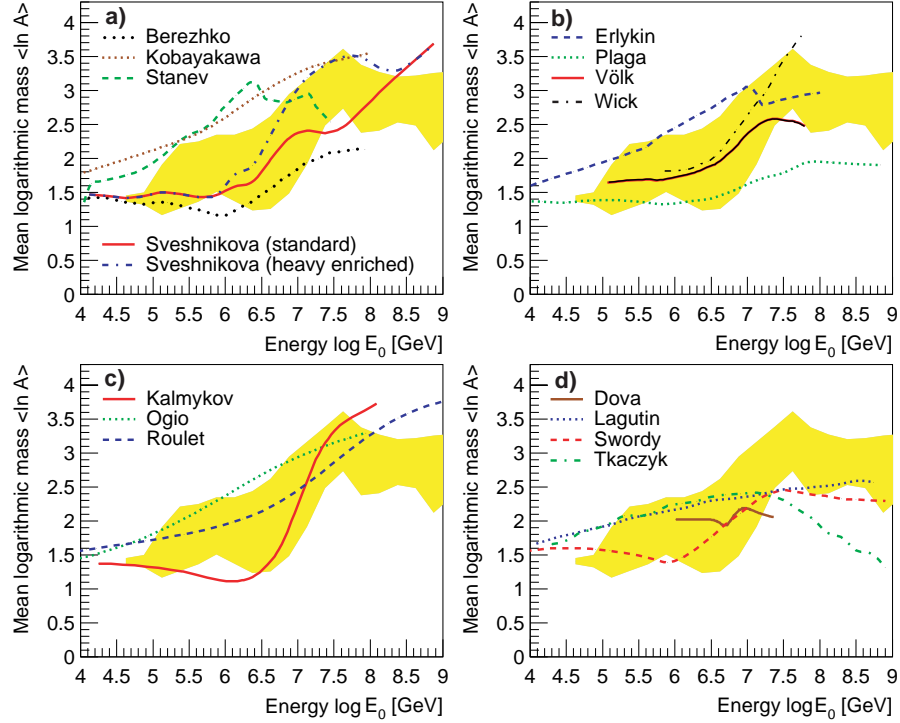


Figure 8: Mean logarithmic mass as function of energy as obtained by various experiments (shaded area) compared with different models (lines). a) Acceleration in SNR (Berezhko et al. [10], Stanev et al. [11], Kobayakawa et al. [12], Sveshnikova et al. [13]); b) Single source model (Erlykin & Wolfendale [14]), acceleration in  $\gamma$ -ray bursts (Plaga [15], Wick et al. [16]), reacceleration in the galactic wind (Völk et al. [22]); c) Diffusion in Galaxy (Kalmykov et al. [38], Ogio et al. [18], Roulet et al. [19]); d) Propagation in the Galaxy (Lagutin et al. [21], Swordy [20]) and interaction with background photons (Tkaczyk [23]) and neutrinos (Dova et al. [24]). For details see [27].

in Fig. 7b [39]. These values follow better the trend of the observations of particles at the ground, shown in Fig. 7c.

Combining the experimental values from Fig. 7b and c, the result is displayed as grey band in Fig. 8. The experimental data are going to be compared to various models, which are discussed in the literature as possible origin of the knee [27].

Several approaches to model the shock acceleration in SNRs (Berezhko et al. [10], Kobayakawa et al. [12], Stanev et al. [11], Sveshnikova et al. [13]) are summarized in Fig. 8a. The models differ in assumptions of properties of the SNRs like magnetic field strength, available energy etc. This yields differences in  $\langle \ln A \rangle$ , as can be inferred from the figure.

Predictions of the single source model (Erlykin & Wolfendale [14]), reacceleration in the galactic wind (Völk et al. [22]) and acceleration in  $\gamma$ -ray bursts (Plaga [15], Wick et al. [16]) are shown in Fig. 8b. The latter differ in their interpretation of the origin for the knee, Plaga attributes it to the maximum energy reached during the acceleration process, while Wick et al. propose leakage from the Galaxy as the cause.

The propagation of cosmic rays as described in diffusion models (Kalmykov et al. [38], Ogio et al. [18], Roulet et al. [19]) yields  $\langle \ln A \rangle$ -values presented in Fig. 8c. They are all based on the approach by Ptuskin et al. [17], but take into account different assumptions on details of the propagation process, like the structure of galactic magnetic fields etc.

The last panel (Fig. 8d) summarizes predictions of models taking into account cosmic-ray propagation in the Galaxy (Lagutin [21], Swordy [20]) as well as interactions with background photons (Tkaczyk [23]) and neutrinos (Dova et al. [24]).

As can be inferred from Fig. 8, the situation is not yet conclusive, but a trend towards a standard picture can be recognized. Some of the proposed explanations can already be excluded. Interactions with background particles in the Galaxy would produce a big amount of secondary protons, which results in a light mass composition at high energies, not confirmed by the experiments. Furthermore, a massive neutrino, proposed in [24] is excluded by measurements of the WMAP and 2dFGRS experiments [40]. The approach described in [15] does not describe the trend of the data. The data are consistent with acceleration in SNRs (Fig. 8a) and diffusive propagation (Fig. 8c). Also reacceleration in the galactic wind (Völk et al.) and acceleration in  $\gamma$ -ray bursts in combination with diffusive propagation (Wick et al.) follow the trend indicated by the data.

## 5 Conclusions

Comparing the present results to the status before the start of the KASCADE experiment (about one decade ago), our knowledge about high-energy cosmic rays has significantly improved. The experiment has shown that the knee is caused by the subsequent cut-offs of individual elements, starting with protons and helium nuclei and that the mean logarithmic mass increases as function of energy.

Summarizing the large number of experimental observations, there are indications for a standard picture of galactic cosmic rays. At least a large fraction of them seems to be accelerated in supernova remnants up to ener-

gies of  $Z \cdot (0.1 - 5)$  PeV. Higher energies may be reached by reacceleration in the galactic wind or by acceleration in additional sources, such as  $\gamma$ -ray bursts. The particles propagate in a diffusive process through the Galaxy. With rising energy the pathlength decreases and particles escape easier from the Galaxy. This brings about the knee in the energy spectrum.

When the understanding of the hadronic interactions in the atmosphere improves, the measurements can be interpreted with higher reliability. This will put more restrictions on the models to describe acceleration and propagation of cosmic rays.

## Acknowledgments

The author acknowledges valuable scientific discussions with his colleagues from the KASCADE-Grande and TRACER experiments. He thanks the organizers of the Vulcano workshop for their invitation, the great hospitality, and the interesting scientific program.

## References

- [1] G.V. Kulikov et al., *J. Exp. Theor. Phys.* 35 (1958) 635
- [2] J.R. Hörandel, *Astropart. Phys.* 19 (2003) 193
- [3] T.G. Guzik et al., *Adv. Space Res.*, in press 2004
- [4] F. Gahbauer et al., *ApJ* 607 (2004) 333
- [5] S.P. Wakely et al., *Nucl. Instr. and Meth.*, in press (2004)
- [6] J.R. Hörandel, *Nucl. Phys. B (Proc. Suppl.)* 122 (2003) 455
- [7] W. Baade and F. Zwicky, *Phys. Rev.* 46 (1934) 76
- [8] E. Fermi, *Phys. Rev.* 75 (1949) 1169
- [9] R.D. Blanford and J.P. Ostriker, *ApJ* 221 (1978) L29
- [10] E.G. Berezhko and L.T. Ksenofontov, *JETP* 89, 3 (1999) 391
- [11] T. Stanev et al., *Astron. & Astroph.* 274 (1993) 902
- [12] K. Kobayakawa et al., *Phys. Rev. D* 66 (2002) 083004 and preprint astro-ph/0008209
- [13] L.G. Sveshnikova, *Astron. & Astroph.*, 409 (2003) 799
- [14] A.D. Erlykin and A.W. Wolfendale, *J. Phys. G: Nucl. Part. Phys.* 27 (2001) 1005
- [15] R. Plaga, *New Astronomy* 7 (2002) 317
- [16] S.D. Wick et al., *Astropart. Phys.* 21 (2004) 125
- [17] V.S. Ptuskin et al., *Astron. & Astroph.* 268 (1993) 726.
- [18] S. Ogio and F. Kakimoto, *Proc. 28th Int. Cosmic Ray Conf., Tsukuba* 1 (2003) 315
- [19] R. Roulet, preprint astro-ph/0310367
- [20] S.P. Swordy, *Proc. 24th Int. Cosmic Ray Conf., Rome* 2 (1995) 697
- [21] A.A. Lagutin et al., *Nucl. Phys. B (Proc. Suppl.)* 97 (2001) 267

- [22] H.J. Völk and V.N. Zirakashvili, Proc. 28th Int. Cosmic Ray Conf., Tsukuba 4 (2003) 2031
- [23] S. Karakula and W. Tkaczyk, Astropart. Phys. 1 (1993) 229
- [24] M.T. Dova et al., preprint astro-ph/0112191
- [25] J. Candia et al., Astropart. Phys. 17 (2002) 23
- [26] D. Kazanas and A. Nicolaidis, preprint astro-ph/0103147
- [27] J.R. Hörandel, Astropart. Phys. 21 (2004) 241
- [28] F. Aharonian et al., Astron. & Astroph. 370 (2001) 112
- [29] E.G. Berezhko et al., Astron. & Astroph. 400 (2003) 971
- [30] A. Chilingarian et al., ApJ 597 (2003) L129
- [31] Kascade Coll.: T. Antoni et al., ApJ 608 (2004) 865
- [32] Kascade Coll.: T. Antoni et al., ApJ 604 (2004) 687
- [33] J. Candia et al., J. Cosmol. Astropart. Phys., 5 (2003) 3
- [34] KASCADE Coll.: H. Ulrich et al., European Physical Journal C (2004) DOI: 10.1140/epjcd/s2004-03-1632-2; K.-H. Kampert et al., Acta Physica Polonica B 35 (2004) 1799; J.R. Hörandel et al., preprint aspro-ph/0311478.
- [35] KASCADE Coll.: T. Antoni et al., ApJ, in press (2004); M. Müller et al., Proc. 28th Int. Cosmic Ray Conf., Tsukuba 1 (2003) 101
- [36] G. Navarra et al., Proc. 28th Int. Cosmic Ray Conf., Tsukuba 1 (2003) 147; S. Valchierotti et al., Proc. 28th Int. Cosmic Ray Conf., Tsukuba 1 (2003) 151
- [37] D. Heck et al., Report FZKA 6019, Forschungszentrum Karlsruhe 1998;  
and <http://www-ik.fzk.de/~heck/corsika>.
- [38] N.N. Kalmykov and A.I. Pavlov, Proc. 26th Int. Cosmic Ray Conf., Salt Lake City 4 (1999) 263
- [39] J.R. Hörandel, J. Phys. G: Nucl. Part. Phys 29 (2003) 2439
- [40] S. Hannestad, preprint astro-ph/0303076